Annals of R.S.C.B., ISSN: 1583-6258, Vol. 25, Issue 1, 2021, Pages. 5399 - 5414
Received 15 December 2020; Accepted 05 January 2021.

Three dimensional Couette flow of Dusty Fluid through a Porous Plate in the presence of Transverse Electrically Conducting Magneto Hydrodynamic Model

K. Rajesh[1], A. Govindarajan[2], M. Vidhya[3]

[1,2]Department of Mathematics, College of Engineering and Technology,

SRM Institute of science and technology, Kattankulathur-603 203,

Kancheepuram District, Tamil Nadu, India.

[3]Department of Mathematics, Sathyabama Institute of science and technology

Tamilnadu, India

Email: Rajeshrose92@gmail.com, Govindarajan.A@ktr.srmuniv.ac.in , mvidhya_1978@yahoo.co.in

*Corresponding Author: A. Govindarajan

Abstract

This paper analyzed the effects of magneti field and dust parameters on the three-dimensional flow of an incompressible viscous dusty fluid past a porous plate under the following conditions: (i) The dusty fluid is electrically conducting (ii) The free stream velocity is uniform (iii) The plate is subjected to a periodic suction velocity distribution (iv) The plate temperature is constant (v) A magnetic field of uniform strength is applied in the direction normal to the plate. The problem is solved by using perturbation method. Solutions are obtained for the velocity field, temperature (both fluid and dust) and skin friction. The effects of Hartmann number (M), suction parameter (α) and dust parameters (f and Λ) on the velocity field and skin friction are discussed with the help of graph and tables. The velocity profiles of both the fluid and dust increase with an increase of either suction parameter (or) Hartmann number (M).

Keywords - Hartmann Number, Reynolds number, Prandtl number, suction parameter, porous medium, permeability parameter, relaxation time and mass concentration.

1. Introduction

The problematic of MHD laminar flow through a porous medium has become very important in recent years particularly in the fields of agricultural engineering to study the underground water resources, seepage of water in river beds, in chemical engineering for filtration and purification process; in petroleum technology to study the movement of natural gas, oil and water through the oil reservoirs. MHD flow with heat transfer has been a subject of interest of many researchers because of its varied application in science and technology. Such phenomena are observed in buoyancy induced motions in the atmosphere, water bodies, quasi-solid bodies such as earth, and so forth. Many industrial applications use magneto hydrodynamics (MHD) effects to resolve the complex problems that very often occurred in industries. The available hydrodynamics solutions include the effects of magnetic field which is possible as the most of the industrial fluids are electrically conducting. Ahmed [1] studied about Magnetic field effect on a three-dimensional mixed convective flow with mass transfer along an infinite vertical porous plate.Loganathan et.al [2] analyzed. Unsteady Three-Dimensional MHD Dusty Couette Flow through Porous Plates with Heat Source. Dey [3] discussed Viscoelastic fluid flow through an annulus with relaxation, retardation effects and external heat source/sink. Ali et al [4] discussed. A report on fluctuating free convection flow of heat absorbing viscoelastic dusty fluid past in a horizontal channel With MHD effect. Israel-Cookey et al [5] investigated MHD

Annals of R.S.C.B., ISSN: 1583-6258, Vol. 25, Issue 1, 2021, Pages. 5399 - 5414
Received 15 December 2020; Accepted 05 January 2021.

oscillatory Couette flow of a radiating viscous fluid in a porous medium with periodic wall temperature. Prasannakumara[6] presented Three-dimensional boundary layer flow and heat transfer of a dusty fluid towards a stretching sheet with convective boundary conditions.Mallikarjuna et.al [7] studied about Three-dimensional boundary layer flow and heat transfer of a fluid particle suspension over a stretching sheet embedded in a porous medium. Manjunatha et.al [8] investigated Thermal analysis of conducting dusty fluid flow in a porous medium over a stretching cylinder in the presence of non-uniform source/sink..Shehzad et.al [9] discussed. Three-dimensional MHD flow of Casson fluid in porous medium with heat generation. Butt et.al [10] analyzed Three-dimensional flow of a magnetohydrodynamic Casson fluid over an unsteady stretching sheet embedded into a porous medium. Mahanthesh et.al [11] presented Nonlinear radiative heat transfer in MHD three-dimensional flow of water based nanofluid over a non-linearly stretching sheet with convective boundary condition.Mishra et.al [12] analyzed. Mass and heat transfer effect on MHD flow of a visco-elastic fluid through porous medium with oscillatory suction and heat source. Mahanthesh et.al [13] studied. Nonlinear convection in nano Maxwell fluid with nonlinear thermal radiation: A three-dimensional study. Veer Krishna, et.al [14] investigated Unsteady MHD reactive flow of second grade fluid through porous medium in a rotating parallel plate channel.Seth et.al [15] investigated Effects of Hall current on unsteady MHD convective Couette flow of heat absorbing fluid due to accelerated movement of one of the plates of the channel in a porous medium.Kumar et.al [16] analysed. Combined influence of fluctuations rotating porous medium with cubic auto-catalysis chemical reaction..Krishna et.al [17] analysed. Hall and ion slip effects on MHD rotating flow of elastico-viscous fluid through porous medium.Ghadikolaei, et.al [18] analyzed MHD boundary layer analysis for micropolar fluid containing nanoparticles over a porous medium. Govindarajan et.al [19] reported on 3D coquette flow of dusty fluid through transpiration cooling. Das et.al [20] investigated the effect of heat source on MHD in the slip flow regime. Vidhya et.al [21] about laminar convection through porous medium between two vertical parallel plates with heat source. Govindarajan et.al [22] discussed the chemical reaction effects on unsteady MHD free convective flow in a rotating porous medium with mass transfer.

In above studies the investigators have confined themselves to two dimensional flows. Bu Yet there may emerge circumstances where the flow fields might be essentially three dimensional. Through the current paper an attempt has been made to study the impact of dust parameters on the three-dimensional MHD dusty flow past a porous plate. The goal of this current paper is to examine the impact of the injection / suction parameter in the three-dimensional MHD duty flow past a porous plate using two-phase fluid. The aim of this section is to study the effect of injection parameter, dust parameters on the velocity field, temperature field and skin friction. The resolution of the present paper is to study the hydro magnetic effects of electrically leading three-dimensional flow of viscous incompressible dusty fluid through a porous medium which is bounded by an infinite vertical porous plate with periodic suction at constant temperature.

A. Mathematical Modelling:

Consider three – dimensional flow of a viscous incompressible dusty fluid through a highly porous medium which is bounded by a vertical infinite porous plate. We choose a co-ordinate system with plate lying vertically on x* - z* plane such that x* axis is taken along the plate in the direction of the flow and is taken along the plate in the direction of the flow and y* axis is ⊥r to the plane of the plate and directed in to the fluid which is flowing with free stream velocity U. All physical quantities will be independent of x*, however the flow remains 3 dimensional due to the variation of the suction velocity distribution of the form $V^*(z^*) = -V\left[1+\varepsilon \cos\left(\frac{\pi z^*}{L}\right)\right]$, the negative sign in the above equation indicates that the suction is towards the plate. Denoting the velocity components of the fluid by u*, v* w* and that of the dust particles by u_p^*, v_p^*, w_p^* respectively, temperature of the fluid by T*

Annals of R.S.C.B., ISSN: 1583-6258, Vol. 25, Issue 1, 2021, Pages. 5399 - 5414
Received 15 December 2020; Accepted 05 January 2021.

and that of the dust by T_p*, the equations which govern the problem are:

Equation of continuity for fluid phase

$$\frac{\partial v^*}{\partial y^*}+\frac{\partial w^*}{\partial z^*}=0 \tag{1}$$

Equation of motion in x-direction within fluid phase

$$v^*\frac{\partial u^*}{\partial y^*}+w^*\frac{\partial v^*}{\partial z^*}=v\left(\frac{\partial^2 u^*}{\partial y^{*2}}+\frac{\partial^2 u^*}{\partial z^{*2}}\right)-\frac{\sigma B_0{}^2 u^*}{\rho}+\frac{KN_0}{\rho}(u_p{}^*-u^*) \tag{2}$$

Equation of motion in y-direction within fluid phase

$$v^*\frac{\partial v^*}{\partial y^*}+w^*\frac{\partial v^*}{\partial z^*}=-\frac{1}{\rho}\frac{\partial p^*}{\partial y^*}+v\left(\frac{\partial^2 v^*}{\partial y^{*2}}+\frac{\partial^2 v^*}{\partial z^{*2}}\right)+\frac{KN_0}{\rho}(v_p{}^*-v^*) \tag{3}$$

Equation of motion in z-direction within fluid phase

$$v^*\frac{\partial w^*}{\partial y^*}+w^*\frac{\partial w^*}{\partial z^*}=-\frac{1}{\rho}\frac{\partial p^*}{\partial y^*}+v\left(\frac{\partial^2 w^*}{\partial y^{*2}}+\frac{\partial^2 w^*}{\partial z^{*2}}\right)-\frac{\sigma B_0{}^2 w^*}{\rho}+\frac{KN_0}{\rho}(w_p{}^*-w_p) \tag{4}$$

The energy equation is

$$\rho C_p\left(v^*\frac{\partial T^*}{\partial y^*}+w^*\frac{w^*\partial^* T^*}{\partial z^*}\right)=k\left(\frac{\partial^2 T^*}{\partial y^{*2}}+\frac{\partial^2 T^*}{\partial z^{*2}}\right)+\mu\varphi+\frac{N_0 m C_s}{\tau_T}(T_p{}^*-T^*) \tag{5}$$

Where $\phi = 2\left[\left\{\left(\frac{\partial v^*}{\partial y^*}\right)^2+\left(\frac{\partial w^*}{\partial y^*}\right)^2\right\}+\left(\frac{\partial u^*}{\partial y^*}\right)^2+\left(\frac{\partial w^*}{\partial y^*}+\frac{\partial w^*}{\partial z^*}\right)^2+\left(\frac{\partial u^*}{\partial z^*}\right)^2\right]$

Equation of continuity in particle phase

$$\frac{\partial v_p{}^*}{\partial y^*}+\frac{\partial w_p{}^*}{\partial z^*}=0 \tag{6}$$

Equation of motion in x-direction within particle phase

$$v_p{}^*\frac{\partial u_p{}^*}{\partial y^*}+w_p{}^*\frac{\partial u_p{}^*}{\partial z^*}=\frac{KN_0}{\rho}(u^*-u_p{}^*) \tag{7}$$

Equation of motion in y-direction within particle phase

$$v_p{}^*\frac{\partial v_p{}^*}{\partial y^*}+w_p{}^*\frac{\partial v_p{}^*}{\partial z^*}=\frac{KN_0}{\rho}(v^*-v_p{}^*) \tag{8}$$

Annals of R.S.C.B., ISSN: 1583-6258, Vol. 25, Issue 1, 2021, Pages. 5399 - 5414
Received 15 December 2020; Accepted 05 January 2021.

Equation of motion in z-direction within particle phase

$$v_p * \frac{\partial w_p *}{\partial y *} + w_p * \frac{\partial w_p *}{\partial z *} = \frac{KN_0}{\rho}(w * - w_p *) \tag{9}$$

The energy equation is

$$v_p * \frac{\partial T_p *}{\partial y *} + w_p * \frac{\partial T_p *}{\partial z *} = -\frac{(T_p * - T*)}{\tau_T} \tag{10}$$

B. The boundary conditions of the problem are:

$y^* = 0$: $u^* = 0$, $v^* = -(1+\varepsilon \cos\left(\frac{\pi z *}{L}\right))$, $w^* = 0$, $T^* = T_w^*$, $u_p^* = 0$, $v_p^* = (1+\varepsilon \cos\left(\frac{\pi z *}{L}\right))$, $T_p^* = T_w^*$, $w_p^* = 0$, $y \to \infty$: $u^* = U$, $P^* = P^*_\infty$, $T = T^*_\infty$, $u^*_p = U$, $T_p = T_\infty^*$, $w^* = 0$, $w_p^* = 0$ (11)

Where β_0 is the magnetic field component along y* - axis C_p is specific heat of the fluid at constant pressure. g is acceleration due to gravity, k is Thermal conductivity of the fluid, K* is permeability of the porous medium, L is Half wave length of the periodic suction velocity, M is Hartmann number, p* is dimensional pressure, T_w* is temperature of the plate, T_∞* is Temperature of the fluid for away from the plate, U is free stream velocity, V is basic steady distribution, ρ is density of the fluid, v is Kinematic viscosity, μ is viscosity of the fluid, α is suction parameter, K is Stokes drag constant which is given by '$6\pi\mu$ a' where 'a' is the radius of the dust particles, f is mass concentration of the dust particles, m is mass of the dust particles, N_0 is Number density of the dust particles assumed to be constant,. Nu is Nusselt number, P is Non dimensional pressure and Pr is Prandtl number.

We presently present the accompanying non-dimensional variables:

$$y = \frac{y *}{L}, z = \frac{z *}{L}, u = \frac{u *}{U}, v = \frac{v *}{U}, w = \frac{w *}{U}, P = \frac{P *}{\rho U^2}, \theta = \frac{T * - T\infty *}{Tw * - T\infty}, u_p = \frac{u_p *}{U}, v_p = \frac{v_p *}{U},$$

$$w_p = \frac{w_p *}{u}, \theta_p = \frac{T_p * - T\infty *}{Tw * - T\infty}, R = \frac{UL}{\upsilon}, M = \frac{\sigma B_0^2\, \upsilon L}{U\mu}, \Pr = \frac{\mu C_p}{k}, \ E = \frac{U^2}{C_p\,(Tw * - T\infty *)}, K = \frac{K * U^2}{v^2}, \alpha = \frac{v}{U.} \tag{12}$$

with the help of above non-dimensional variables equations (1) to (10) become.

After introducing the non-dimensional quantities, the equation of motion for fluid phase is obtained as:

Equation of continuity for fluid phase

$$\frac{\partial v}{\partial y} + \frac{\partial w}{\partial z} = 0 \tag{13}$$

Equation of motion in x-direction within fluid phase

$$v\frac{\partial u}{\partial y} + w\frac{\partial u}{\partial z} = \frac{1}{R}\left(\frac{\partial^2 u}{\partial y^2} + \frac{\partial^2 u}{\partial z^2}\right) - Mu + \frac{f}{\Lambda}(u_p - u) \tag{14}$$

Equation of motion in y-direction within fluid phase

Annals of R.S.C.B., ISSN: 1583-6258, Vol. 25, Issue 1, 2021, Pages. 5399 - 5414
Received 15 December 2020; Accepted 05 January 2021.

$$v\frac{\partial v}{\partial y}+w\frac{\partial v}{\partial z}=-\frac{\partial p}{\partial y}+\frac{1}{R}\left(\frac{\partial^2 v}{\partial y^2}+\frac{\partial^2 v}{\partial z^2}\right)+\frac{f}{\Lambda}(v_p-v) \tag{15}$$

Equation of motion in z-direction within fluid phase

$$v\frac{\partial w}{\partial y}+w\frac{\partial w}{\partial z}=-\frac{\partial p}{\partial z}+\frac{1}{R}\left(\frac{\partial^2 w}{\partial y^2}+\frac{\partial^2 w}{\partial z^2}\right)-Mw+\frac{f}{\Lambda}(w_p-w) \tag{16}$$

The energy equation is

$$v\frac{\partial \theta}{\partial y}+w\frac{\partial \theta}{\partial z}=\frac{1}{R\Pr}\left(\frac{\partial^2 \theta}{\partial y^2}+\frac{\partial^2 \theta}{\partial z^2}\right)+\frac{E}{R}\varphi+\frac{2f}{3\Lambda\Pr}(\theta_p-\theta) \tag{17}$$

where $\phi = 2\left\{\left(\frac{\partial v}{\partial y}\right)^2+\left(\frac{\partial w}{\partial z}\right)^2\right\}+\left\{\left(\frac{\partial u}{\partial y}\right)^2+\left(\frac{\partial w}{\partial y}+\frac{\partial v}{\partial z}\right)^2+\left(\frac{\partial u}{\partial z}\right)^2\right\}$

After introducing the non-dimensional quantities, the equation of motion for particle phase is obtained as

Equation of continuity for particle phase:

$$\frac{\partial v_p}{\partial y}+\frac{\partial w_p}{\partial z}=0 \tag{18}$$

Equation of motion in x-direction within particle phase

$$v_p\frac{\partial u_p}{\partial y}+w_p\frac{\partial u_p}{\partial z}=\frac{1}{\Lambda}(u-u_p) \tag{19}$$

Equation of motion in y-direction within particle phase

$$v_p\frac{\partial v_p}{\partial y}+w_p\frac{\partial v_p}{\partial z}=\frac{1}{\Lambda}(v-v_p) \tag{20}$$

Equation of motion in z-direction within particle phase

$$v_p\frac{\partial w_p}{\partial y}+w_p\frac{\partial w_p}{\partial z}=\frac{1}{\Lambda}(w-w_p) \tag{21}$$

The energy equation is

$$v_p\frac{\partial \theta_p}{\partial y}+w_p\frac{\partial \theta_p}{\partial z}=\frac{2}{3\Pr\Lambda\gamma}(\theta-\theta_p) \tag{22}$$

The corresponding boundary conditions become:

$y = 0$: $u = 0$; $v = -\alpha(1+\varepsilon\cos\pi z)$, $w = 0$, $\theta = 1$, $u_p = 0$, $v_p = \alpha(1+\varepsilon\cos\pi z)$, $w_p = 0$, $\theta_p = 1$, $y \to \infty$:

Annals of R.S.C.B., ISSN: 1583-6258, Vol. 25, Issue 1, 2021, Pages. 5399 - 5414
Received 15 December 2020; Accepted 05 January 2021.

$u = 1$, $P = P_\infty$, $w = 0$, $\theta = 0$, $u_p = 1$, $w_p = 0$,

$\theta_p = 0$. (23)

In order to solve these differential equations we assume that $f(y, z) = f_0(y) + \varepsilon f_1(y, z)$, (24)

Where f is suitably replaced by u, u_p, v, v_p, w, w_p, θ, θ_p, P. With the help of (24) substituting in equations (13) to (22) and equating the terms free from ε, we get the following system of differential equations.

$$u_0^{11} + \alpha R\, u_0^1 - MRu_0 + \frac{fR}{\Lambda}(u_{p_0} - u_0) = 0 \tag{25}$$

$$\theta_0^{11} + \mathrm{Re}\,\mathrm{Pr}\,\theta_0^1 + \frac{2fR}{3\Lambda}(\theta_{p_0} - \theta_0) = -E\,\mathrm{Pr}\,u_0^{12} \tag{26}$$

$$(\alpha D - b_1)\theta_{p0} + b_1\,\theta_0 = 0 \tag{27}$$

$$(\Lambda\alpha\, D + 1)\ u_{p0} = u_0 \tag{28}$$

Where Prime denotes he differentiation with respect to 'y'.

The corresponding boundary conditions become

y= 0: $u_0 = 0$; $v_0 = -\alpha$, $w_0 = 0$, $\theta_0 = 1$, $u_{p0} = 0$, $v_{p0} = \alpha$,

$w_{p0} = 0$, $\theta_{p0} = 1$ $y \to \infty$: $u_0 = 1$, $p_0 = P_\infty$, $w_0 = 0$, $\theta_0 = 0$, $u_{p0} = 1$, $w_{p0} = 0$, $\theta_{p0} = 1$. (29)

The solutions of equations (25) to (28) are $v_0 = -\alpha$, $v_{p0} = \alpha$, $w_0 = 0$, $w_{p0} = 0$, $p_0 = p_\infty$, $u_0 = 1 - e^{-my}$,

$$u_{p0} = \frac{\alpha\Lambda m\, e^{-}\left(\frac{y}{\Lambda\alpha}\right) - e^{-my}}{1 - \alpha\Lambda m} + 1, \quad \theta_0 = e^{-noy} + E_1(e^{-2my} - e^{-noy})$$

$$\theta_{po} = E_1 b_1\left[\frac{e^{-2my} - e^{\frac{-b1y}{\alpha\Lambda}}}{b_1 - 2m\alpha\Lambda} + \frac{e^{\frac{-b_1y}{\Lambda\alpha}} - e^{-noy}}{b_1 - n_0\alpha\Lambda}\right] + \left[\frac{b_1 e^{-noy} - \alpha n_o \Lambda e^{-\left(\frac{b_1 y}{\alpha\Lambda}\right)}}{b_1 - \alpha n_o \Lambda}\right] \tag{30}$$

When we equate the coefficient ε we get the succeeding system of differential equations.

$$\frac{\partial v_1}{\partial y} + \frac{\partial w_1}{\partial z} = 0 \tag{31}$$

$$v_p \frac{\partial u_0}{\partial y} - \alpha\frac{\partial u_1}{\partial y} = \frac{1}{R}\left(\frac{\partial^2 u_1}{\partial y^2} + \frac{\partial^2 u_1}{\partial z^2}\right) - Mu_1 + \frac{f}{\Lambda}(u_{p_1} - u_1) \tag{32}$$

Annals of R.S.C.B., ISSN: 1583-6258, Vol. 25, Issue 1, 2021, Pages. 5399 - 5414
Received 15 December 2020; Accepted 05 January 2021.

$$-\alpha\frac{\partial v_1}{\partial y}=-\frac{\partial p_1}{\partial y}+\frac{1}{R}\left(\frac{\partial^2 v_1}{\partial y^2}+\frac{\partial^2 v_1}{\partial z^2}\right)+\frac{f}{\Lambda}(v_{p1}-v_1) \tag{33}$$

$$-\alpha\frac{\partial w_1}{\partial y}=-\frac{\partial p_1}{\partial y}+\frac{1}{R}\left(\frac{\partial^2 w_1}{\partial y^2}+\frac{\partial^2 w_1}{\partial z^2}\right)-Mw_1+\frac{f}{\Lambda}(w_{p1}-w_1) \tag{34}$$

$$-\alpha\frac{\partial \theta_1}{\partial y}+v_1\frac{\partial \theta_0}{\partial y}=\frac{1}{\operatorname{Re}\Pr}\left(\frac{\partial^2 \theta_1}{\partial y^2}+\frac{\partial^2 \theta_1}{\partial z^2}\right)+\frac{2E}{R}u_0^1\frac{\partial u_1}{\partial y}+\frac{2f}{3\Lambda\Pr}(\theta_{p1}-\theta_1) \tag{35}$$

$$\frac{\partial v_{p1}}{\partial y}+\frac{\partial w_{p1}}{\partial z}=0 \tag{36}$$

$$\alpha\frac{\partial u_{p1}}{\partial y}+v_{p1}\frac{\partial u_{p0}}{\partial y}=\frac{1}{\Lambda}(u_1-u_{p1}) \tag{37}$$

$$\alpha\frac{\partial v_{p1}}{\partial y}=\frac{1}{\Lambda}(v_1-v_{p1}) \tag{38}$$

$$\alpha\frac{\partial w_{p1}}{\partial y}=\frac{1}{\Lambda}(w_1-w_{p1}) \tag{39}$$

$$v_{p1}\theta_{P0}^1+\alpha\frac{\partial \theta_{p1}}{\partial y}=-b_1\,(\theta_{P1}-\theta_1) \tag{40}$$

The parallel boundary conditions become:

$y = 0$: $u_1 = 0$; $v_1 = -\alpha \cos \pi z$, $w_1 = 0$, $\theta_1 = 0$, $u_{p1} = 0$, $v_{p1} = \alpha \cos \pi z$, $w_{p1} = 0$, $\theta_{p1} = 0$, $y\theta_1 = 0$, $u_{p1} = 0$,

$w_{p1} = 0$,

$\theta_{p1} = 0$. (41)

In order to solve equations (33, 34, 38) and (39) we assume that

$v_1 (y,z) = v_{11} (y) \cos \pi z$ (42)

$w_1(y,z) = -\frac{1}{\pi}v_{11}^1(y)\sin \pi z,$ (43)

$p_1 (y,z) = P_{11} (y) \cos \pi z$ (44)

$v_{p1} = v_{P11} (y) \cos \pi z$ (45)

Annals of R.S.C.B., ISSN: 1583-6258, Vol. 25, Issue 1, 2021, Pages. 5399 - 5414
Received 15 December 2020; Accepted 05 January 2021.

$$w_{p1} = -\frac{1}{\pi} w_{p_{11}}^{1} (y) \sin \pi z \tag{46}$$

On substituting these equations in equations (33), (34), (38) & (39) we get the following equations:

$$\left\{ D^2 + R\alpha D - (\pi^2 + \frac{fR}{\Lambda}) \right\} v_{11} + \frac{fR}{\Lambda} v_{p11} = RP_{11}^1 \tag{47}$$

$$(\alpha D\Lambda+1)\, v_{p11} + v_{11} = 0 \tag{48}$$

$$\left\{ D^3 + R\alpha D^2 - (\pi^2 + MR + \frac{fR}{\Lambda})D \right\} v_{11} + \frac{fR}{\Lambda} v_{p11} = R\pi^2 p_{11} \tag{49}$$

$$(\alpha D^2\Lambda+D)\, v_{p11} + v^1_{11} = 0 \tag{50}$$

Equations (42), (43), (44) and (46) are so chosen such that the continuity equations (31) and (36) are satisfied.

The parallel boundary conditions become

$y = 0$: $v_{11} = -\alpha$, $v^1_{11} = 0$, $v_{p11} = \alpha$, $v_p{}^1{}_{11} = 0$,

$y \to \infty$: $v_{11} = 0$, $v_{p11} = 0$, $v^1_{11} = 0$, $v^1_{p11} = 0$, $p_{11} = 0$ (51)

On solving equations (47) (48), (49) & (50) under the transformed boundary conditions (51)

we get,

$$v_1 = \frac{\alpha}{r_2 - r_3} \left[r_3\, e^{-r_2 y} - r_2\, e^{-r_3 y} \right] \cos \pi\, z, \tag{52}$$

$$w_1 = \frac{\alpha\, r_2 r_3}{\pi(\, r_2 - r_3)} \left[\, e^{-r_2 y} - e^{-r_3 y} \right] \sin \pi\, z, \tag{53}$$

$$v_{p1} = \frac{\alpha}{(r_2 - r_3)} \left[\frac{r_3 e^{-r_2 y}}{1 - r_2 \Lambda \alpha} - \frac{r_2 e^{-r_3 y}}{1 - r_3 \Lambda \alpha} \right] \cos \pi\, z, \tag{54}$$

$$w_{p1} = \frac{\alpha\, r_2\, r_3}{\pi(r_2 - r_3)} \left[\frac{e^{-r_2 y}}{1 - r_2 \Lambda \alpha} - \frac{e^{-r_3 y}}{1 - r_3 \Lambda \alpha} \right] \sin \pi\, z, \tag{55}$$

In order to solve (32), (35), (37), (40) we assume that

$$u_1 (y,z) = u_{11} (y) \cos \pi z \tag{56}$$

$$\theta_1 (y,z) = \theta_{11} (y) \cos \pi z \tag{57}$$

$$u_{p1} (y,z) = u_{p11} (y) \cos \pi z \tag{58}$$

Annals of R.S.C.B., ISSN: 1583-6258, Vol. 25, Issue 1, 2021, Pages. 5399 - 5414
Received 15 December 2020; Accepted 05 January 2021.

$\theta_{p1}(y,z) = \theta_{p11}(y)\cos \pi z$ (59)

On substituting (56), (57), (58) & (59) in (32), (35), (37) & (40) we get the following equations:

$$\left\{D^2 + \alpha RD - (\pi^2 + MR + \frac{fR}{\Lambda}\right\} u_{11} + \frac{fR}{\Lambda} u_0^1 = R\, v_{11}\, u_0^1 \quad (60)$$

$$(\Lambda\alpha D + 1)\, u_{p11} + u_{11} = v_{p11}\, u_{p0}^1 \quad (61)$$

$$\left\{D^2 + \alpha R \Pr D - (\pi^2 + \frac{2f\,\mathrm{Re}}{3\Lambda})\right\} \theta_{11} + \frac{2f\,\mathrm{Re}}{3\Lambda} \theta p_{11} = \mathrm{Re}\Pr \theta_0^1\, v_{11} - 2E\Pr u_{11}^1 u^1{}_0 \quad (62)$$

$$(\alpha D + b_1)\, \theta p_{11} + b_1 \theta_{11} = v_{p11}\, \theta_{p0}^1 \quad (63)$$

The corresponding boundary conditions become:

$y = 0$: $u_{11} = 0$; $\theta_{11} = 0$, $u_{p11} = 0$, $\theta_{p11} = 0$, $y \to \infty$:

$u_{11} = 0$, $\theta_{11} = 0$, $u_{p11} = 0$, $\theta_{p11} = 0$ (62)

On solving equations (60), (61),(62)&(63) under the boundary conditions (64), we get

$$u = (1 - e^{-my}) + \frac{\in R\alpha m}{(r_2 - r_3)}\begin{bmatrix} A_1\, e^{-(m+r_3)y} - \\ A_2\, e^{-(m+r_2)y} + A_3\, e^{-r_4 y} \end{bmatrix}\cos \pi z \quad (65)$$

$$u_p = \frac{(\alpha\Lambda m\, e^{-\frac{y}{\Lambda\alpha}} - e^{-my})}{1 - \alpha\Lambda m} + 1 + \in \left\{ C\, e^{-\frac{y}{\Lambda\alpha}} + \frac{R\alpha m}{(r_2 - r_3)}\left[\frac{A_1\, e^{-(m+r_3)y}}{1 - \alpha\Lambda(m + r_3)} - \frac{A_2\, e^{-(m+r_3)y}}{1 - \alpha\Lambda(m + r_2)} + \frac{A_3\, e^{-r_a y}}{1 - r_4\Lambda\alpha}\right]\right.$$
$$\left. + \frac{\alpha\Lambda m}{(r_2 - r_3)(1 - \alpha\Lambda m)}\frac{r_3}{(1 - r_2\Lambda\alpha)}\left\{\frac{e^{-(r_2+m)y}}{1 - \alpha\Lambda(r_2 + m)} + \frac{e^{-(r_2 + \frac{1}{\Lambda\alpha})y}}{\alpha\Lambda r_2}\right\}\left[-\frac{r_2}{(1 - r_3\Lambda\alpha)}\left\{\frac{e^{-(r_3+m)y}}{1 - \alpha\Lambda(m + r_3)} + \frac{e^{-(r_3 + \frac{1}{\Lambda\alpha})y}}{\alpha\,\Lambda\, r_3}\right\}\right]\right\} \cos\pi z \quad (66)$$

Where r_1, r_2, r_3, r_4, r_5, A_1, A_2, I_1, I_2, S_1, S_2, S_3, S_4, S_5, t_1, t_2, P_1,P_2, P_3, g_1, g_2, g_3, g_4, g_5, g_6, PI_1, PI_2, PI_3, are given in Appendix-A Realizing the velocity field we can acquire the articulations for the shear stress segments in the x* and z* directions in the non-dimensional structure as::

$$Tx = \frac{Tx^*}{\rho UV} = \frac{\upsilon}{VL}\left(\frac{du}{dy}\right)_{y=0} = m + \frac{\in R\alpha m}{(r_2 - r_3)}\left[-A_1(m + r_3) + A_2(m + r_2) - A_3\, r_4\right]\cos \pi z \quad (67)$$

$$Tx = \frac{Tz^*}{\left(\mu\frac{V}{L}\right)} = \frac{U}{V}\left(\frac{dw}{dy}\right)_{y=0} = \frac{\in \alpha\, r_2\, r_3}{\pi}\sin \pi z \quad (70)$$

$$\mathrm{Nu} = \frac{dq^* W}{k(T_0 - T_1)} = \left(\frac{d\theta}{dy}\right)_{y=0}$$

Annals of R.S.C.B., ISSN: 1583-6258, Vol. 25, Issue 1, 2021, Pages. 5399 - 5414
Received 15 December 2020; Accepted 05 January 2021.

Results and Discussion

The effects of varying the Hartmann number (M), Suction parameter (α) and Mass concentration (f). With R = 1, z = 0, $\Lambda = 0.2$ and $\in = 0.2$ on velocity and skin friction are shown in fig-1 to fig-5 and table-1.

A) Main flow velocity profiles of the Fluid Phase

The velocity profiles of the dusty fluid in main flow direction are shown in fig-1. From fig-1 we see that irrespective of any value of (α) suction parameter and (M) Hartmann number the profiles increase with an increase in the mass concentration of the dust particles. Also the profiles increase with an increase in the Hartmann number (M) for any value of the mass concentration of the dust particles. It is interesting to note that the profiles increase with an increase of the suction parameter (α) for any value of the mass concentration (f) and Hartmann number (M). All the profiles increase steadily near the lower plate and attain its maximum value very near the lower plate and thereafter it becomes linear and reaches the value 1 at the other plate.

B) Main flow velocity profiles of the Particle Phase

The velocity profile of the dust in the main flow direction is shown in fig-2 & fig-3. From fig-2 we conclude that the velocity profiles of the dust particles increase with an increase of either the mass concentration of the dust particles (f) (or) suction parameter (α), (or) Hartmann number (M). The velocity profiles increase steadily near the lower plate and reaches its maximum value very near the lower plate and thereafter it becomes linear and reach the value 1 at the other plate

By comparing the velocities of both the fluid and dust we conclude that both the profiles behave in the same manner. The profiles of the fluid are at a lower height as compared with the dust. The velocity increases up to y = 2 and then after it becomes linear.

In the case of clean fluid (f = 0) the velocity profiles increase with the increase of Hartmann number (M) and suction parameter (α) both. It is also noted the in the case of clean fluid, the velocity increases up to y = 4 and then after it becomes linear. This phenomenon can be attributed to the presence of dust. So we can say that the presence of dust has an influence of accelerating the motion of the fluid.

C) Cross flow velocity profiles

The cross flow velocity component W_1 is due to the transverse sinusoidal suction velocity distribution applied through the porous plate at rest. The secondary flow component is shown in fig-4 & fig-5. It is interesting to note from fig-4 & fig-5 that (W_1) the cross flow velocity increases with an increase in the Hartmann number (M) irrespective any value of the mass concentration of the dust particles and suction parameter (α). Also it is noted that the profiles maintain the same increasing trend with an increase in the suction parameter for any value of Hartmann number (M) and mass concentration of the dust particles. All the profiles increase steadily near the lower plate and thereafter reverse its trend and become 1 at the other plate. The profiles have greater height for greater value of the suction parameter. From fig-5 it is observed that the profiles increase with an increase in the mass concentration of the dust particles irrespective any value of Hartmann number (M) and suction parameter (α).

The variations of the skin friction components Tx and Tz in the main flow and transverse directions and shown in Table-1. From Table-1 we conclude that for a given value of the mass concentration, relaxation time of the dust particles and suction parameter, both Tx and Tz increase with an increase in the Hartmann number. Both Tx and Tz increase with an increase in the mass concentration of the dust particles, irrespective of any value of

Annals of R.S.C.B., ISSN: 1583-6258, Vol. 25, Issue 1, 2021, Pages. 5399 - 5414
Received 15 December 2020; Accepted 05 January 2021.

Hartmann number (M) and suction parameter (α). Both Tx and Tz increase with an increase in the suction parameter for any value of Hartmann number (M) and mass concentration (f).

But in the case of the clean fluid (f = 0) Tx increases with an increase of suction parameter (α) in the absence of magnetic field but in the presence of magnetic field it decreases. This is due to the presence of dust and dust an influence in one of the skin friction coefficient

For clean fluid (f = 0), Tz decreases with the increase of magnetic field. But for dusty fluid the skin friction component Tz behaves in opposite manner. This can be said that dust plays an important role in changing the skin friction component Tz when the concentration parameter of the dust particles is neglected it has been found that our results are in perfect agreement with the results obtained by G.D Gupta and Rajesh Johari in their paper

Variations of Hartmann number, Mass Concentration & suction parameter for main flow velocity profiles of u (y,z) in fig -1.

Figures and Tables

$\alpha = 0.5$			$\alpha = 1.0$		
Curve	M	f	Curve	M	f
1	0	0.2	7	0	0.2
2	0	0.4	8	0	0.4
3	2	0.2	9	2	0.2
4	2	0.4	10	2	0.4
5	4	0.2	11	4	0.2
6	4	0.4			

Fig-1. Main flow velocity profiles of the fluid u(y,z) for z = 0, Λ = 0.2 and various values of Hartmann number (M), Mass concentration (f) and Suction parameters (α).

Annals of R.S.C.B., ISSN: 1583-6258, Vol. 25, Issue 1, 2021, Pages. 5399 - 5414
Received 15 December 2020; Accepted 05 January 2021.

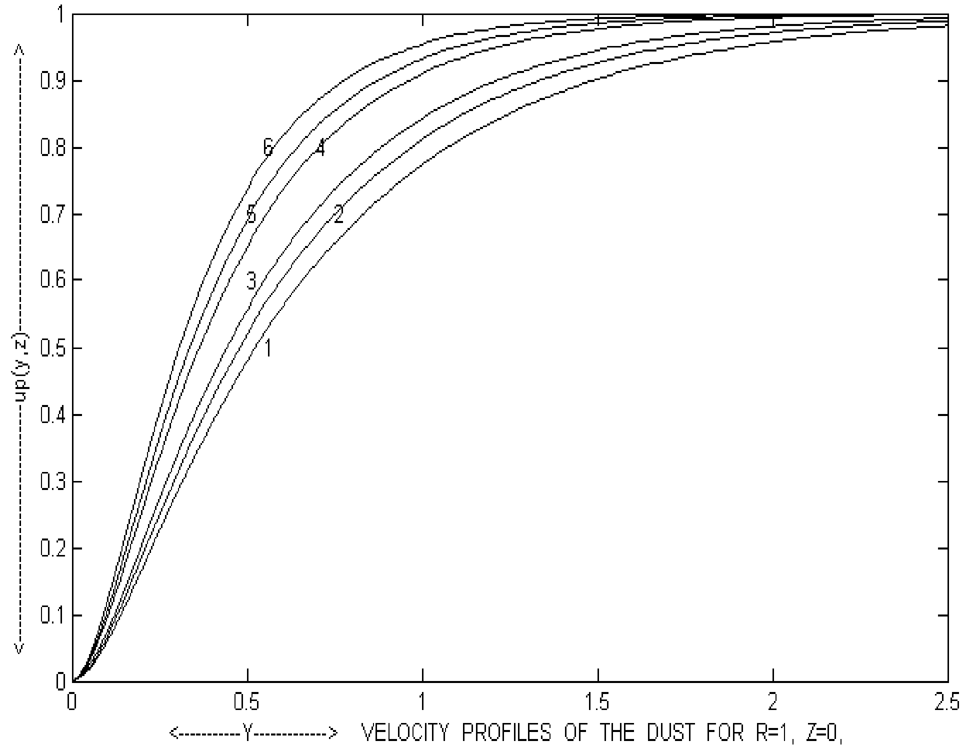

Fig-2. Main flow velocity profiles of the dust u_p (y, z) for z =0, Λ = 0.2 and various values of Hartmann number (M), Mass concentration (f) and Suction parameters (α)

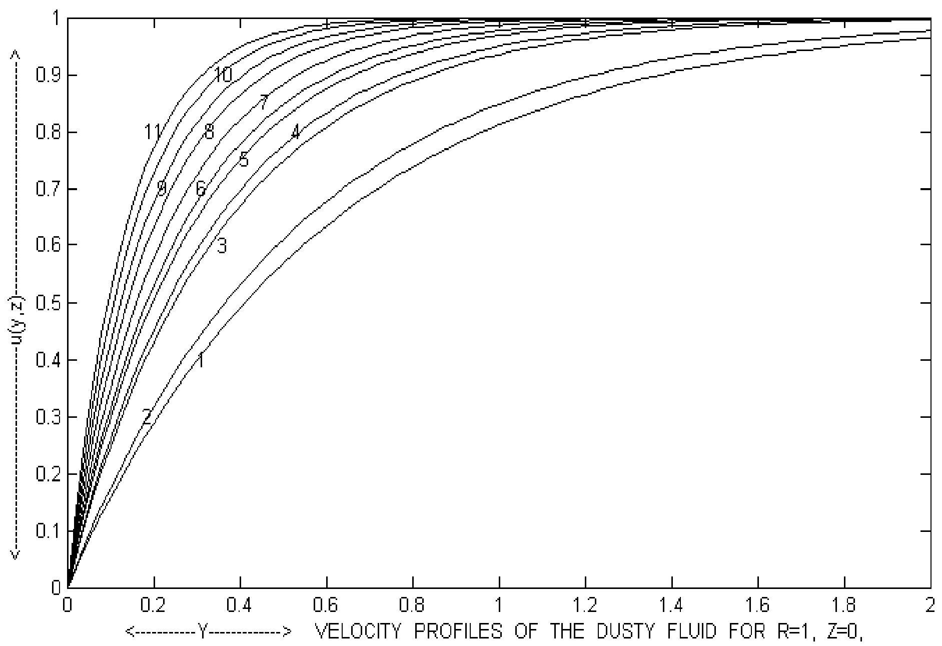

Fig-3. Main flow velocity profiles of the dust u_p (y, z) for z = 0, Λ = 0.2 and various values of Hartmann number (M), Mass concentration (f) and Suction parameters (α).

Annals of R.S.C.B., ISSN: 1583-6258, Vol. 25, Issue 1, 2021, Pages. 5399 - 5414
Received 15 December 2020; Accepted 05 January 2021.

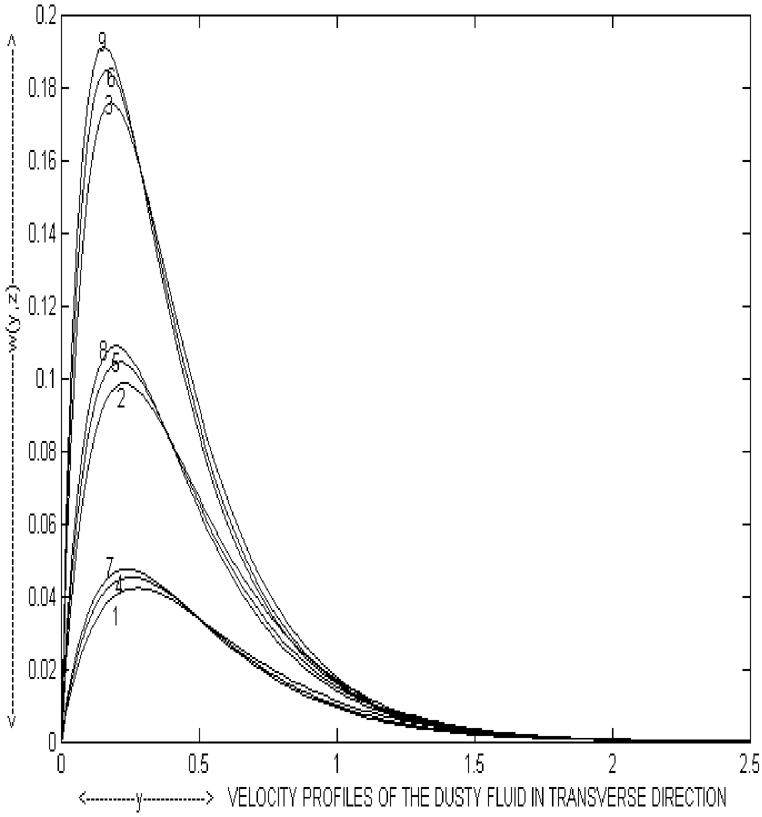

Fig-4. Cross flow velocity profiles of the fluid w (y, z) for z = 0.5, Λ = 0.2, f = 0.2 and various values of Hartmann number (M) and Suction parameters (α).

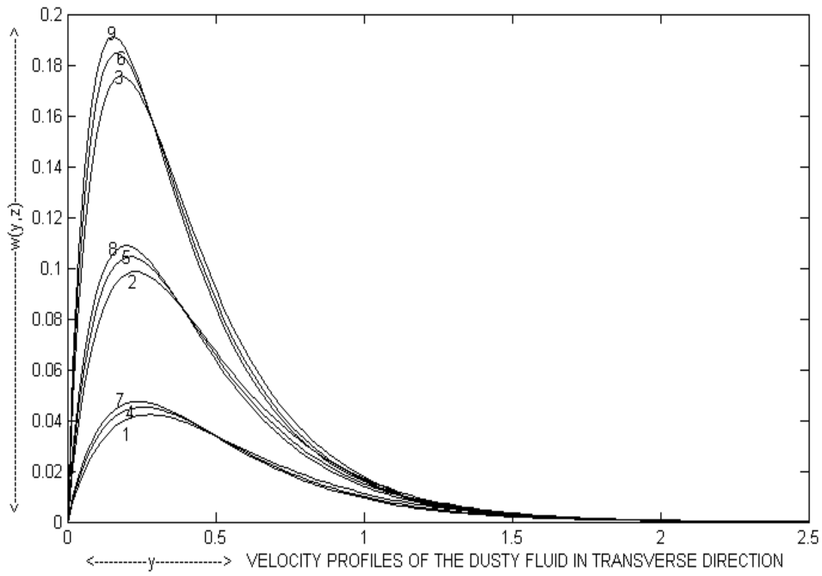

Variations of Mass Concentration parameter for cross flow velocity profiles of w(y,z) when M = 0 and α 0.

Annals of R.S.C.B., ISSN: 1583-6258, Vol. 25, Issue 1, 2021, Pages. 5399 - 5414
Received 15 December 2020; Accepted 05 January 2021.

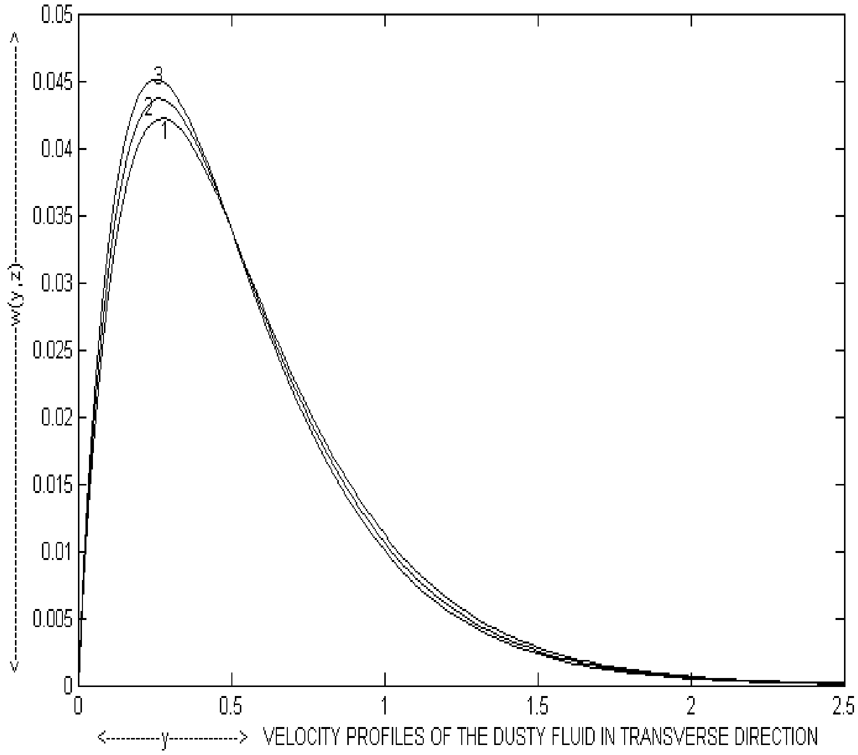

Fig-5. Cross flow velocity profiles of the fluid w (y, z) for z = 0.5, Λ = 0.2, α = 0.5 M = 0 and various values of Mass concentration parameter (f).

F	M=0		M=2		M=4	
α=0.5	Tx	Tz	Tx	Tz	Tx	Tz
0.2	1.6809	2.0878	2.7814	2.4431	3.4916	2.6990
0.4	1.7836	2.1197	2.8369	2.4698	3.5432	2.7257
0.6	1.8889	2.1520	2.9129	2.4973	3.6136	2.7530
α=1.0	Tx	Tz	Tx	Tz	Tx	Tz
0.2	3.8571	5.8893	5.0324	6.8282	5.9681	7.6222
0.4	4.0756	6.0669	5.2239	6.9937	6.1576	7.7860
0.6	4.3010	6.2478	5.4246	7.1631	6.3525	7.9533
α=1.5	Tx	Tz	Tx	Tz	Tx	Tz
0.2	7.1727	13.4600	8.6359	15.6421	9.9509	17.5763
0.4	7.4577	14.0194	8.9761	16.1718	10.3176	18.0964
0.6	7.8544	14.5863	9.3622	16.7107	10.7045	18.6252

Annals of R.S.C.B., ISSN: 1583-6258, Vol. 25, Issue 1, 2021, Pages. 5399 - 5414
Received 15 December 2020; Accepted 05 January 2021.

6. Conclusion

In main flow velocity profile of the dust fluid and velocity profile of particle phase increases when there is an increase in the mass concentration of the dust particles.as the result of velocity profiles increase steadily near the lower plate and reaches its maximum value very near the lower plate and thereafter it becomes linear and reach the value 1 at the other plate.in dusty fluid velocity profile increase in the increase of Hartmann number(M) and Suction parameters (α) up to y=2 and it becomes liner whereas the same trend follows in the clean fluid (f=0) then the velocity becomes linear up to y=4. So, we can say that the presence of dust has an influence of accelerating the motion of the fluid. The cross-flow velocity increases with an increase whenever Hartmann number (M) and suction parameter (α) increases in both clean and dust fluid.in clean fluid f=0 T_X increases with increase in suction parameter (α) in the absence of magnetic field but T_X decreases with increase in suction parameter (α)in the presence of magnetic field. In the presence of magnetic field. T_Z decrease for clean fluid f=0 and T_Z behaves oppositely in the dust fluid.

References

[1] N. Ahmed Magnetic field effect on a three-dimensional mixed convective flow with mass transfer along an infinite vertical porous plat Int. J. Eng. Sci. Tech., 2 (2) (2010), pp. 117-135
[2] Loganathan, C., and S. Gomathi. "Unsteady Three-Dimensional MHD Dusty Couette Flow through Porous Plates with Heat Source." Asian Journal of Applied Sciences (ISSN: 2321 – 0893) Volume 04 – Issue 06, December 2016
[3] Dey, D., 2018. Viscoelastic fluid flow through an annulus with relaxation, retardation effects and external heat source/sink. Alexandria Engineering Journal, 57(2), pp.995-1001.
[4] Ali, F., Bilal, M., Gohar, M., Khan, I., Sheikh, N.A. and Nisar, K.S., 2020. A report on fluctuating free convection flow of heat absorbing viscoelastic dusty fluid past in a horizontal channel With MHD effect. Scientific Reports, 10(1), pp.1-15. 8
[5] Israel-Cookey, C., Amos, E. and Nwaigwe, C., 2010. MHD oscillatory Couette flow of a radiating viscous fluid in a porous medium with periodic wall temperature. Am. J. Sci. Ind. Res, 1(2), pp.326-331.
[6] BC, Prasannakumara, and Shashikumar NS. "Three-dimensional boundary layer flow and heat transfer of a dusty fluid towards a stretching sheet with convective boundary conditions." Journal of Computational & Applied Research in Mechanical Engineering (JCARME) 8(1) pp.25-38, (2018)
[7] Mallikarjuna, H. B., M. C. Jayaprakash, and Raghavendra Mishra. "Three-dimensional boundary layer flow and heat transfer of a fluid particle suspension over a stretching sheet embedded in a porous medium." Nonlinear Engineering 8(1) pp.734-743,2019
[8] Manjunatha, Pattasale Thippeswamy, Bijjanal Jayanna Gireesha, and Ballajja Chandrappa Prasannakumara. "Thermal analysis of conducting dusty fluid flow in a porous medium over a stretching cylinder in the presence of non-uniform source/sink." International journal of mechanical and materials engineering 9(1)pp.1-10.2014..
[9] Shehzad, S. A., T. Hayat, and A. Alsaedi. "Three-dimensional MHD flow of Casson fluid in porous medium with heat generation." Journal of Applied Fluid Mechanics 9, no. 1 (2016): 215-223.
[10] Butt, A. S., M. N. Tufail, and Asif Ali. "Three-dimensional flow of a magnetohydrodynamic Casson fluid over an unsteady stretching sheet embedded into a porous medium." Journal of Applied Mechanics and Technical Physics 57, no. 2 (2016): 283-292.
[11] Mahanthesh, B., B. J. Gireesha, and Rama Subba Reddy Gorla. "Nonlinear radiative heat transfer in MHD three-dimensional flow of water based nanofluid over a non-linearly stretching sheet with convective boundary condition." Journal of the Nigerian Mathematical Society 35, no. 1 (2016): 178-198.
[12] Mishra, S. R., G. C. Dash, and M. Acharya. "Mass and heat transfer effect on MHD flow of a visco-elastic

Annals of R.S.C.B., ISSN: 1583-6258, Vol. 25, Issue 1, 2021, Pages. 5399 - 5414
Received 15 December 2020; Accepted 05 January 2021.

fluid through porous medium with oscillatory suction and heat source." International Journal of Heat and Mass Transfer 57, no. 2 (2013): 433-438.

[13] Mahanthesh, B., B. J. Gireesha, G. T. Thammanna, S. A. Shehzad, F. M. Abbasi, and R. S. R. Gorla. "Nonlinear convection in nano Maxwell fluid with nonlinear thermal radiation: A three-dimensional study." Alexandria Engineering Journal 57, no. 3 (2018): 1927-1935.

[14] VeeraKrishna, M., and G. Subba Reddy. "Unsteady MHD reactive flow of second grade fluid through porous medium in a rotating parallel plate channel." The Journal of Analysis 27, no. 1 (2019): 103-120.

[15] Seth, Gauri Shanker, Rohit Sharma, and Bidyasagar Kumbhakar. "Effects of Hall current on unsteady MHD convective Couette flow of heat absorbing fluid due to accelerated movement of one of the plates of the channel in a porous medium." Journal of Porous Media 19, no. 1 (2016).

[16] Kumar, Rakesh, and Shilpa Sood. "Combined influence of fluctuations in the temperature and stretching velocity of the sheet on MHD flow of Cu-water nanofluid through rotating porous medium with cubic auto-catalysis chemical reaction." Journal of Molecular Liquids 237 (2017): 347-360.

[17] Krishna, M. Veera, and Ali J. Chamkha. "Hall and ion slip effects on MHD rotating flow of elastico-viscous fluid through porous medium." International Communications in Heat and Mass Transfer 113 (2020): 104494.

[18] Ghadikolaei, S. S., Kh Hosseinzadeh, M. Hatami, and D. D. Ganji. "MHD boundary layer analysis for micropolar dusty fluid containing Hybrid nanoparticles (Cu-Al2O3) over a porous medium." Journal of Molecular Liquids 268 (2018): 813-823.

[19] A.Govindarajan, V.Ramamurthy and Sundarammal Kesavan, 3D Couette flow of dusty fluid with transpiration cooling, Journal of Zhejiang University-Science A, 8(2), pp 313–322

[20] Das, S. S., et al., Mass Transfer Effects on MHD Flow and Heat Transfer past a Vertical Porous Plate through a Porous Medium under Oscillatory Suction and Heat Source, International Journal of Heat and Mass Transfer, 52 (2009), 25-26, pp. 5962-5969

[21] M.Vidhya and Sundarammal Kesavan, Laminar convection through porous medium between two vertical parallel plates with heat source, International Conference on Frontiers in Automobile and Mechanical Engineering,IEEE Explore,(2010), pp 197-200

[22] A.Govindarajan, A.J. Chamkha, Sundarammal kesavan, M.Vidhya., Chemical reaction effects on unsteady magnet hydrodynamic free convective flow in a rotating porous medium with mass transfer, Thermal Science, 18(2),(2014),pp515-526.